J Mater Sci (2008) 43:2286–2292
DOI 10.1007/s10853-007-2108-6



# Photocatalytic activities of nanocrystalline Si-modified titania xerogels prepared by the glycothermal method

**Hirotaka Ozaki · Kazuko Saito · Shinji Iwamoto · Masashi Inoue**

Received: 7 November 2006 / Accepted: 13 August 2007 / Published online: 22 November 2007


**Abstract** Xerogels of nanocrystalline Si-modified titanias having large surface areas and superior thermal stabilities were obtained by the glycothermal method, followed by the removal of the organic phase by flash evaporation, and their physicochemical and photocatalytic properties were investigated. With the increase in the amount of Si addition, the crystallite size of the sample decreased and BET surface area increased. The zeta potential shifted to the more negative side by Si addition, which affected the adsorbability of dyes. The obtained xerogels of Si-modified titanias were effective photocatalysts for decomposition of organic dyes and exhibited higher activities compared to JRC-TIO-4. Xerogel samples were highly dispersed in aqueous solutions because the coagulation, which may occur during the drying stage in the sample preparation, was effectively prevented and this feature is one of the critical factors for the high activities of the xerogel catalysts. Their effectiveness for photocatalytic decomposition of cationic dyes was remarkable since the negative surface charge of the catalysts enhanced the adsorbability for these dyes.

## Introduction

Semiconductor photocatalysts have attracted great attention because they can be utilized for air purification, water purification, anti-bacteria, self-cleaning materials, etc. Among various photocatalyst materials, titanium dioxide ($TiO_2$) has been most widely used and investigated [1–3], because it has advantages in inexpensiveness, chemical stability, and nontoxicity in addition to its favorable optoelectronic property.

In order to improve the photocatalytic activity of titania photocatalysts, various dopants have been explored. Among them, $SiO_2$ exhibited the most promising results. For example, Tada et al. examined the photocatalytic oxidation of cetylpyridinium bromide in aqueous solutions using $SiO_x/TiO_2$ photocatalysts and reported that the activity was improved with the $SiO_x$ monolayer coverage on the surface of $TiO_2$. They explained the results by the increase in the electrostatic attraction between the catalyst surface and cetylpyridinium ion [4]. Bard et al. found that incorporation of $SiO_2$ to a $TiO_2$-based photocatalyst by a sol–gel method improved photocatalytic activities for the decomposition of Rhodamine 6G and explained that the higher activity of the $TiO_2/SiO_2$ catalysts than bare $TiO_2$ is due to an increase in the amount of the substrate near the catalyst surface [5].

One of the authors, M. I., reported direct synthesis of anatase-type nanocrystalline titanias by thermal reaction of titanium alkoxides in organic media [6–8]. Recently, it was also reported that the thermal reaction of titanium tetraisopropoxide (TIP) and tetraethyl orthosilicate (TEOS) in 1,4-butanediol (glycothermal reaction) afforded nanocrystalline Si-modified titanias with the anatase structure having quite large surface areas and high thermal stabilities [9–11]. Furthermore, xerogels of Si-modified titania were prepared by flash evaporation of the glycothermal solvent, and it was demonstrated that the obtained xerogel catalysts exhibited enhanced activities for photocatalytic oxidation of acetic acid [12]. In this study, Si-modified titania xerogels having higher Si contents were prepared and their

H. Ozaki · K. Saito · S. Iwamoto (✉) · M. Inoue
Department of Energy and Hydrocarbon Chemistry, Graduate School of Engineering, Kyoto University, Katsura, Kyoto 615-8510, Japan
e-mail: iwamoto@scl.kyoto-u.ac.jp

physicochemical properties and photocatalytic activities for degradation of several organic dyes were investigated.

## Experimental

### Preparation of the catalysts

Titania and Si-modified titanias were prepared by the glycothermal method [8]: TIP (25 g) and an appropriate amount of TEOS (Si/Ti atomic ratio of 0–0.5) were added to 100 mL of 1,4-butanediol and this mixture was placed in a 300-mL autoclave. After the atmosphere inside the autoclave was replaced with nitrogen, the assembly was heated to 300 °C at a rate of 2.3 °C/min and kept at that temperature for 2 h. After the glycothermal reaction, the assembly was cooled and the resulting powders were collected by centrifugation, washed with methanol, and then air-dried. The product was calcined in a box furnace in air at 600 °C for 30 min to remove the surface organic moieties. The thus-obtained products are designated as GT($x$), where $x$ is the Si/Ti charged ratio. Xerogel titania and Si-modified titanias were prepared according to the procedure reported previously [12]: After the glycothermal reaction, one of the valves of the autoclave was slightly opened to remove the organic matter in the autoclave by flash evaporation while keeping the autoclave temperature at 300 °C. After all the volatile compounds were eliminated, the autoclave was cooled, and then bulky solid products were directly obtained. The products were calcined in a box furnace in air at 600 °C for 30 min. The thus-obtained products are designated as XG($x$), where $x$ is the Si/Ti charged ratio.

### Characterizations

The UV–vis absorption spectra of the samples were recorded on a Shimadzu MPS-2000 spectrophotometer. Powder X-ray diffraction (XRD) patterns were recorded on a Shimadzu XD-D1 diffractometer using CuK$\alpha$ radiation and a carbon-monochromator. The specific surface areas of the samples were calculated by the BET single-point method on the basis of the nitrogen uptake measured at 77 K. X-ray photoelectron spectroscopy (XPS) measurement was performed on an ULVAC-PHI Model 5500 spectrometer with 15 kV–400 W MgK$\alpha$ emission as the X-ray source. The zeta potentials were measured on an electrophoretic light scattering spectrophotometer, Otsuka Electronics, ELS-800. A small amount of the sample was dispersed in a 10 mmol/L NaCl solution and then pH of the suspension was adjusted by adding 0.1 N NaOH or 0.1 N HCl. The measurement was conducted after ultrasonic treatment of the suspension for 10 min. The particle size distribution was determined by measuring the dynamic light scattering on the same electrophoretic light scattering spectrometer, ELS-800. A portion of the catalyst (20 mg) was added in 100 mL of distilled water and pH of the suspension was adjusted to 5.0 with 0.1 N NaOH or 0.1 N HCl. The measurement was carried out after ultrasonic treatment for 10 min.

### Photocatalytic reaction and adsorption isotherm

Photocatalytic activity was evaluated by degradation of six organic dyes, Rhodamine 6G (Rh6G), Rhodamine B (RhB), Eosin Y (EY), Orange G (OG), Acid Orange 7 (AO7), and Acid Yellow 23 (AY23), whose structures are shown in Fig. 1. Among these dyes, Rh6G and RhB are cationic dyes and other four are anionic dyes. A portion of the catalyst (20 mg) was dispersed in a 100 mL solution of a dye, and the obtained suspension was irradiated with a 500 W high-pressure mercury arc lamp at 25 °C under magnetic stirring. Initial concentrations of the dyes in the solutions were $1.0 \times 10^{-4}$ mol/L for Rh6G and RhB, $2.0 \times 10^{-4}$ mol/L for EY, OG, and AY23, and $3.0 \times 10^{-4}$ mol/L for AO7. After a certain period of irradiation, a portion of the suspension was taken out and filtered. The solution was then analyzed by a UV–vis spectrometer, Shimadzu MPS-2000, to measure the concentration of the remaining organic dye. JRC-TIO-4 (equivalent to Degussa P-25; rutile/anatase = 3/7; BET surface area = 49 $m^2/g$) was used as a reference to compare the photocatalytic activity of the catalysts.

Adsorption isotherms were measured for the suspensions containing 50 mg of the sample and 100 mL of the dye solution with various concentrations. After stirring in the dark for 1 h, the concentration of the dye in the solution was measured with the UV–vis spectrometer.

## Results and discussion

Figure 2 depicted the XRD patterns of XG($x$)s with various Si/Ti ratios, which show that all the products had the anatase structure. The BET surface areas and crystallite sizes of XG($x$)s are listed in Table 1. The crystallite size of XG(0) was 18 nm, and by the addition of a small amount of Si, the crystallite size significantly decreased. With further increase in the amount of Si addition, the crystallite size decreased gradually. For XG(0.5), quite a small crystallite size, 8 nm, was obtained. The BET surface areas increased from 75 $m^2/g$ to 140 $m^2/g$ with the increase in the amount of Si modification up to Si/Ti = 0.2. However, the BET surface area reached a plateau level for Si/Ti = 0.2–0.4,

**Fig. 1** Structures of organic dyes

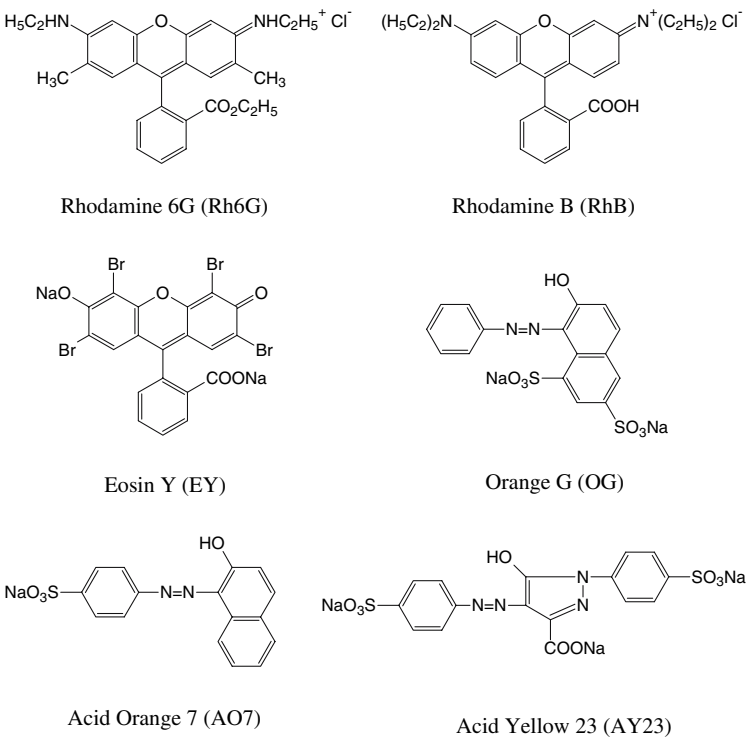


and for XG(0.5) it rather decreased. By increasing the Si/Ti charged ratio, the maximum intensity as well as the area of the XRD peak decreased gradually, suggesting the presence of non-crystalline components in the samples. We have previously examined the surface properties of GT($x$)s by TPD methods and found that GT($x$) samples with $x$ smaller than 0.1 has the surface property similar to that of pure $TiO_2$ and in the case of GT($x$) with $x$ higher than 0.2, a part of the surface was covered with $SiO_2$-like components [10].

The results of XPS of XG($x$)s are shown in Table 2. The Si/Ti ratios of the samples determined by XPS increased with increasing the amount of Si modification. The Si/Ti ratios measured by XPS were always larger than those charged for the glycothermal reaction, indicating that Si was enriched in the surface region of the samples. The O1s XPS spectra of XG($x$)s are shown in Fig. 3. In the O1s XPS spectrum of XG(0), a peak was observed at 530 eV, which corresponds to the oxygen in $TiO_2$. For the Si-modified titanias, another component was recognized at 532 eV. This component is due to the oxygen associated with the Si–O–Ti bridging bond [13, 14]. These results indicate the absence of pure $SiO_2$ clusters on the surface of the product particles, since the O1s peak of oxygen in pure $SiO_2$ is observed at around 533 eV [15].

Figure 4 shows the zeta potentials of XG($x$)s as a function of pH. The isoelectric point of the samples as well as the zeta potentials at pH 5.0 estimated from the results shown in Fig. 4 are listed in Table 1. The isoelectric point

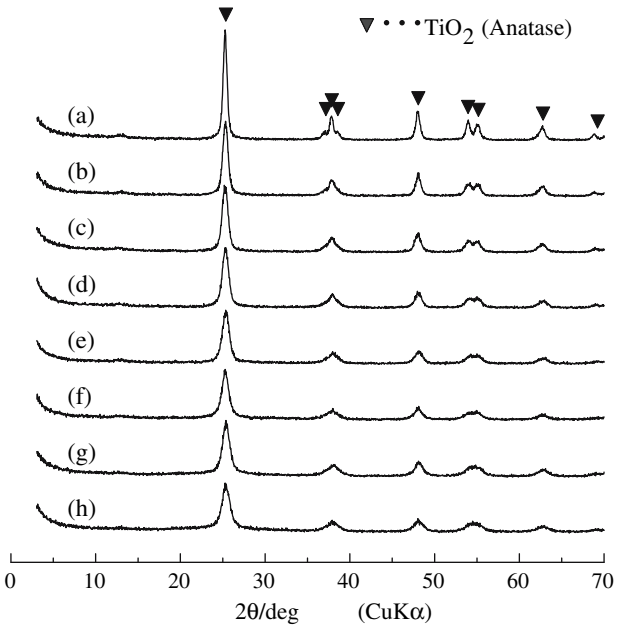


**Fig. 2** XRD patterns of: (**a**) XG(0), (**b**) XG(0.02), (**c**) XG(0.06), (**d**) XG(0.1), (**e**) XG(0.2), (**f**) XG(0.3), (**g**) XG(0.4), and (**h**) XG(0.5)

of XG(0) was around 6.5, and the value gradually shifted to the lower pH side with increasing the amount of Si addition. Since the isoelectric point of pure $SiO_2$ is ca. 2.0 [16], the observed change in the isoelectric point suggests the presence of Si-rich components on the surface of the Si-modified titanias.

**Table 1** Physical properties of the catalysts

| Sample | Crystallite size (nm) | BET surface area ($m^2/g$) | Isoelectric point | Zeta potential[a] (mV) |
|---|---|---|---|---|
| JRC-TIO-4 | – | 49 | 7.0 | 25.4 |
| XG(0) | 20 | 76 | 6.5 | 20.1 |
| XG(0.02) | 16 | 95 | 6.2 | 19.6 |
| XG(0.06) | 13 | 129 | 6.1 | 14.4 |
| XG(0.1) | 11 | 142 | 5.7 | 7.6 |
| XG(0.2) | 10 | 146 | 4.3 | –7.4 |
| XG(0.3) | 9 | 124 | 3.9 | –10.1 |
| XG(0.4) | 9 | 145 | 3.6 | –12.5 |
| XG(0.5) | 8 | 90 | 3.4 | –15.2 |

[a] The value at pH 5

**Table 2** Binding energy of core electrons for XG($x$)s

| Sample | Si/Ti[a] | O1s (eV) | $Si2p_{1/2}$ (eV) | $Ti2p_{3/2}$ (eV) |
|---|---|---|---|---|
| XG(0) | | 529.8 | | 458.7 |
| XG(0.02) | 0.055 | 529.9 (84)[b] | 101.9 | 458.9 |
| | | 531.8 (16) | | |
| XG(0.06) | 0.130 | 530.0 (76) | 102.1 | 458.7 |
| | | 531.8 (24) | | |
| XG(0.1) | 0.171 | 529.9 (71) | 102.1 | 458.7 |
| | | 531.6 (29) | | |
| XG(0.2) | 0.412 | 530.0 (63) | 102.4 | 458.7 |
| | | 532.0 (37) | | |
| XG(0.3) | 0.653 | 530.1 (54) | 102.7 | 458.8 |
| | | 532.1 (46) | | |
| XG(0.4) | 0.748 | 530.2 (52) | 102.9 | 459.0 |
| | | 532.3 (48) | | |
| XG(0.5) | 1.272 | 530.2 (40) | 102.9 | 458.9 |
| | | 532.4 (60) | | |

[a] Determined by XPS

[b] The number in parentheses indicates the percentage of the peak

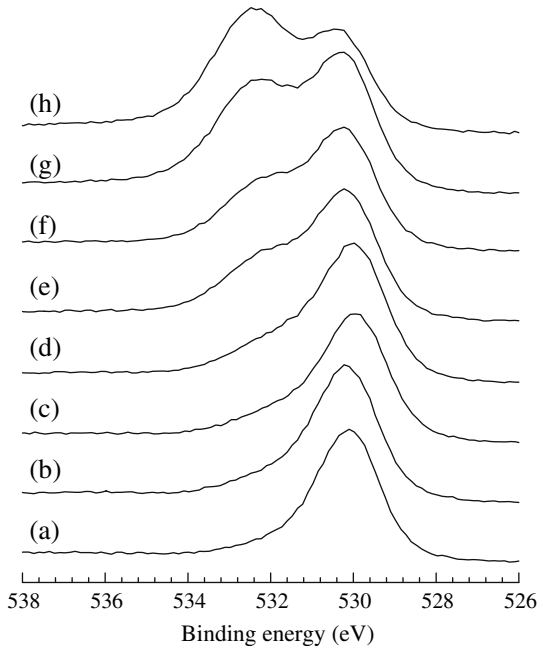


**Fig. 3** O1s XPS spectra of: (**a**) XG(0), (**b**) XG(0.02), (**c**) XG(0.06), (**d**) XG(0.1), (**e**) XG(0.2), (**f**) XG(0.3), (**g**) XG(0.4), and (**h**) XG(0.5)

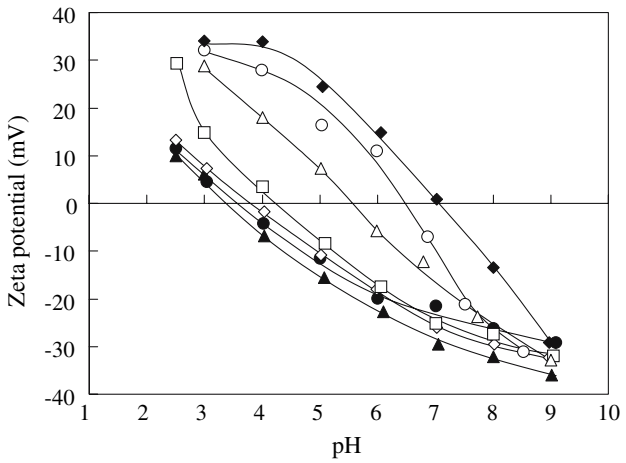


**Fig. 4** Zeta potentials of: (○) XG(0), (Δ) XG(0.1), (□) XG(0.2), (◇) XG(0.3), (●) XG(0.4), (▲) XG(0.5), and (◆) JRC-TIO-4; as a function of pH

Figure 5(a) shows the adsorption isotherms of Rh6G (cationic dye). The amount of Rh6G adsorbed on the samples increased significantly by increasing the Si/Ti charged ratio up to 0.4. The pH values of the diluted Rh6G solutions were 5.0–5.5, and in this pH range, the zeta potential of XG(0) was ca. +20 mV, and it gradually decreased by increasing the Si/Ti ratio. Since Rh6G is a cationic dye that is adsorbed preferably on a negatively charged surface, the enhancement of the Rh6G uptake of the Si-modified titanias is explained by the change in the surface charge. Further increase in the Si/Ti ratio to 0.5 resulted in a slight decrease in the amount of the dye adsorbed. This is probably due to the smaller BET surface area of XG(0.5) than that of XG(0.4). As for the OG (anionic dye) adsorption, the highest amount of adsorption was observed for JRC-TIO-4 and the amount of the adsorption gradually decreased with the increase in the amount of Si addition as shown in Fig. 5(b). This tendency is completely opposite to that of Rh6G, and is also explained by the change in the zeta potentials of the samples.

The amount of the dyes adsorbed on 50 mg of the catalysts from the 100 mL of $2.0 \times 10^{-5}$ mol/L dye solution is shown in Fig. 6 as a function of the Si/Ti charged ratio. For the cationic dyes (RhB and Rh6G), the amounts of the adsorbed dyes markedly increased with the increase in the

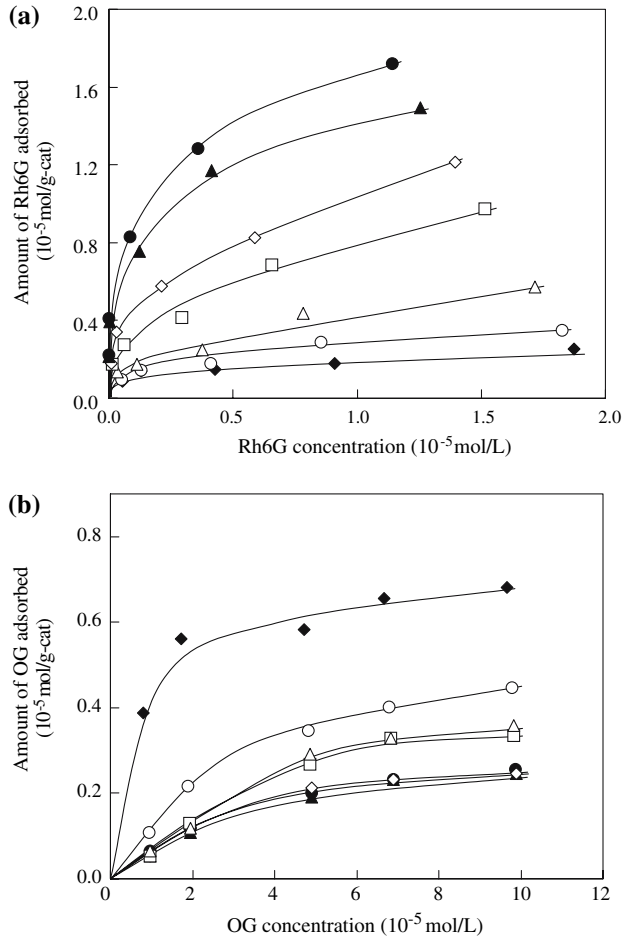


**Fig. 5** Isotherms for adsorption of: (**a**) Rh6G and (**b**) OG; on: (○) XG(0), (Δ) XG(0.1), (□) XG(0.2), (◇) XG(0.3), (●) XG(0.4), (▲) XG(0.5), and (◆) JRC-TIO-4

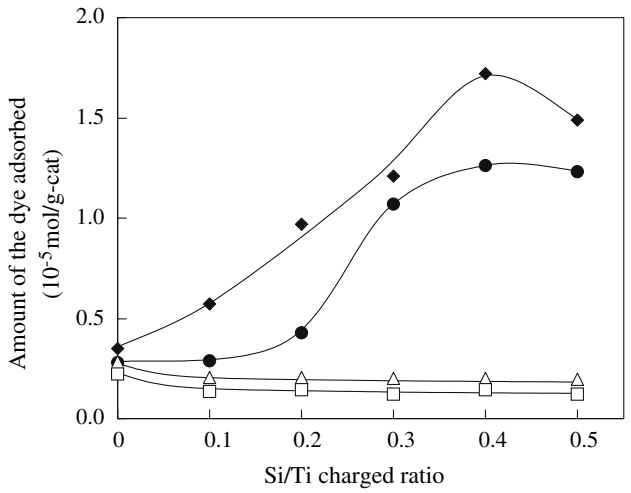


**Fig. 6** Amounts of the dyes: (◆) Rh6G, (●) RhB, (Δ) EY and (□) OG; adsorbed on the Si-modified xerogel catalysts with various Si/Ti charged ratios

Si/Ti ratio. On the other hand, the adsorbed amount of the anionic dyes (EY and OG) decreased. In Fig. 7, the amounts of the dyes adsorbed on the catalysts are plotted as a function of zeta potential at pH 5. The adsorbed amount of the cationic dyes significantly increased, as the zeta potential of the catalyst changed from +20 mV to –15 mV. On the other hand, for the anionic dyes, the amount of adsorption increased slightly as the surface potential increased. The adsorbability of the cationic dyes is influenced strongly by the surface electric charge, while that of anionic dyes is slightly affected.

Figure 8 shows the particle size distributions of XG($x$)s and JRC-TIO-4 in aqueous suspensions at pH 5. For GT($x$) samples, we also conducted the measurement; however, when the ultrasonic irradiation was stopped, the particles in the suspensions began to sediment quickly. This result can be attributed to the coagulation of GT($x$) particles which occurred during the drying stage by the strong surface tension of the liquid between the fine particles. Even with the prolonged ultrasonic treatment, reliable data were not obtained. In the case of JRC-TIO-4, the suspension was milky and relatively stable for several minutes after the ultrasonic treatment, although a small amount of the sediment was recognized after several hours. The measured particle size of JRC-TIO-4 was distributed in a range from 60 nm to 1 μm, as shown in Fig. 8. The crystallite size of this sample, calculated from the XRD peak broadening of the anatase phase, was 31 nm. Therefore, the obtained result suggests that JRC-TIO-4 was comprised of stiff aggregates of smaller primary particles. On the other hand, the suspensions of all of XG($x$)s were quite stable. Especially, XG($x$)s with higher Si/Ti ratios ($x \geq 0.2$) did not sediment even after a couple of days. The suspensions were translucent, which was also quite different from the case of JRC-TIO-4. The turbidity of the suspension is due to the

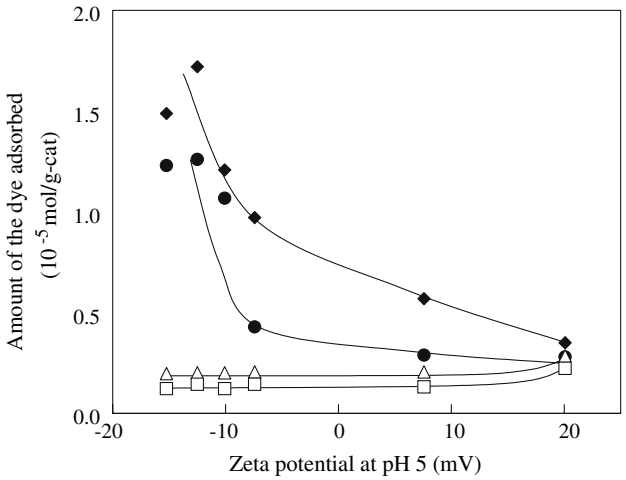


**Fig. 7** Effect of zeta potential of the catalyst on the amount of the dyes adsorbed at pH 5: (◆) Rh6G, (●) RhB, (Δ) EY, and (□) OG

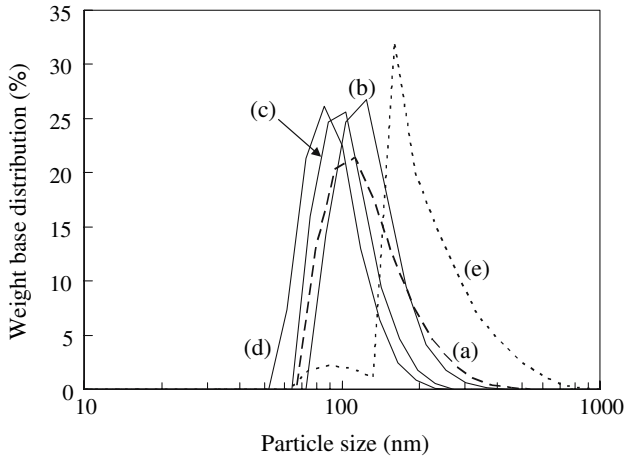


**Fig. 8** Particle size distributions of: (**a**) XG(0), (**b**) XG(0.1), (**c**) XG(0.2), (**d**) XG(0.3), and (**e**) JRC-TIO-4 in aqueous suspensions at pH 5

scattering of visible light by the presence of relatively large particles in the suspension, and therefore, these observations also suggest that XG($x$)s were highly dispersed in the suspension as compared to JRC-TIO-4. Particle sizes of XG(0) measured by the light scattering were ranging from 70 to 550 nm, which was much smaller than that of JRC-TIO-4. By the Si-modification, the particle sizes were further reduced; for examples, 70–450 nm for XG(0.1), 60–300 nm for XG(0.2), and 50–250 nm for XG(0.3). Such high dispersion of XG($x$)s was due to the effective prevention of the coagulation of the ultrafine particles by drying the products via the flash evaporation method.

Figure 9 shows the photocatalytic decomposition of various organic dyes using XG($x$)s. Although $\ln(C/C_0)$ vs. time plots were made in order to compare the decomposition rate, in most of the cases they showed quite complex behaviors and linear relationships were not obtained clearly. This is probably because of ignoring the effect of dye-sensitized photocatalytic reactions, which have been observed in various dye-$TiO_2$ systems [17, 18], or not considering the effect of partially decomposed organic intermediates. Therefore, the photocatalytic activities were simply compared from the concentration of the dyes remaining after 60 min of irradiation. XG(0) showed a photocatalytic activity as high as JRC-TIO-4 for degradation of both the cationic and anionic dyes. The photocatalytic activity for degradation of cationic dyes was improved by increasing the amount of Si modification up to 0.2–0.4. The pH values of the initial suspensions were around 5, and they changed into 4–4.5 after the photocatalytic reaction for 2–3 h. In this pH range, the zeta potential was positive for XG(0) and XG(0.1), and negative

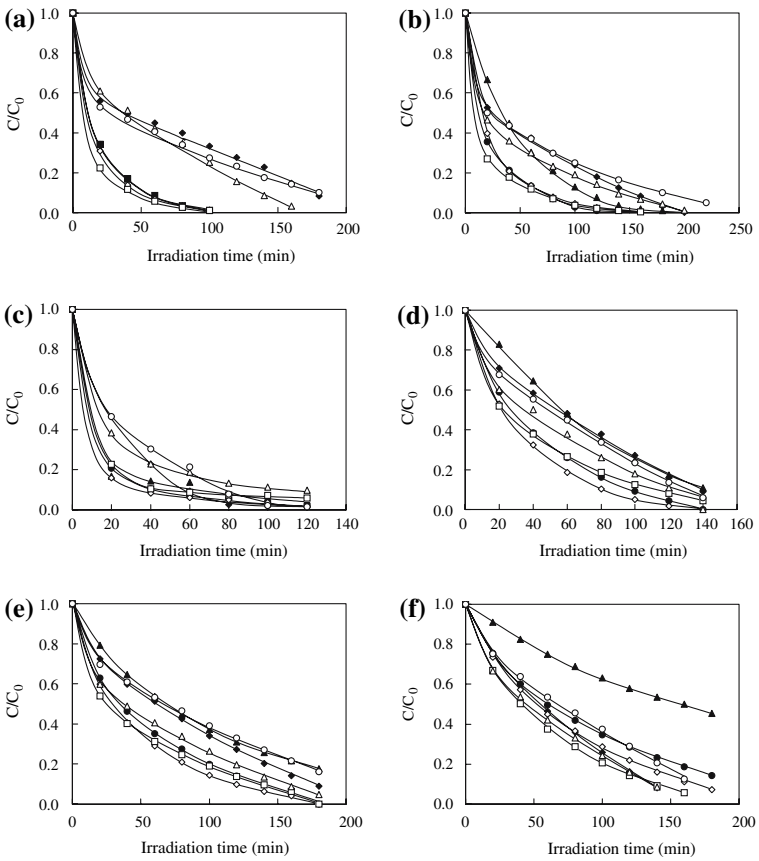


**Fig. 9** Photocatalytic activities of: (○) XG(0), (Δ) XG(0.1), (□) XG(0.2), (◇) XG(0.3), (●) XG(0.4), (▲) XG(0.5), and (◆) JRC-TIO-4; for the decompositions of: (**a**) Rh6G, (**b**) RhB, (**c**) EY, (**d**) OG, (**e**) AO7, and (**f**) AY23

for XG($x$)s with higher $x$. Such surface changes strongly affect adsorption for Rh6G and RhB and lead to the remarkable enhancements of the photocatalytic activities.

For the degradation of anionic dyes, XG($x$)s were also effective and XG(0.2) and XG(0.3) exhibited relatively higher photocatalytic activities. Although the zeta potential varied from +20.1 mV for XG(0) to –15.2 mV for XG(0.5) at pH 5, these changes in zeta potential slightly decreased the adsorbability of anionic dyes. Therefore, the dispersion of the samples seems to be a more important factor for the enhancement of the photocatalytic activity.

For XG(0.5), the photocatalytic activities were relatively low for both the cationic and anionic dyes. These diminished activities are probably due to surface Si-rich components, which are suggested by XPS analysis and BET surface area measurement described in this study as well as the results of TPD reported previously [10].

The obtained results suggest that the adsorption property as well as the particle size distribution (dispersibility) of the sample affected the photocatalytic activity for decomposition under the experimental condition in this study.

## Conclusions

Xerogels of Si-modified titanias prepared by the glycothermal method were effective for photocatalytic decomposition of various organic dyes. As the amount of Si modification increased, the isoelectric point shifted to the lower pH side and the surface of the catalysts in the suspension became more negatively charged. This increased the adsorption for the cationic dyes and led to the enhancement of the decomposition rate. On the other hand, for the anionic dyes, the negative side shift of the zeta potential slightly decreased the dye uptake of the catalysts. However, enhanced photocatalytic activities were observed for the catalysts with small amounts of Si, and the high dispersibility of xerogel catalysts seems to be the reason for the higher photocatalytic activities of Si-modified titanias.

**Acknowledgements** This study was supported by a Grant-in-Aid for Scientific Research (No. 16510085) from Ministry of Education, Culture, Sports, Science and Technology, Japan, and by Kansai Research Foundation for Technology Promotion. One of the authors, H. O., thanks research fund from Iketani Science and Technology Foundation.

## References

1. Fujishima A, Rao TN, Tryk DA (2000) J Photochem Photobiol C 1:1
2. Hoffman MR, Martin ST, Choi W, Bahnemann DW (1995) Chem Rev 95:69
3. Carp C, Huisman CL, Reller A (2004) Prog Solid State Chem 32:33
4. Tada H, Akazawa M, Kubo Y, Ito S (1998) J Phys Chem B 102:6360
5. Anderson C, Bard AJ (1995) J Phys Chem 99:9882
6. Inoue M (2005) Chemical processing of ceramics, 2nd edn. Taylor & Francis, Boca Raton, FL, p 21
7. Inoue M (2004) J Phys: Condens Matter 16:S1291
8. Inoue M, Kominami H, Otsu H, Inui T (1991) Nippon Kagaku Kaishi (J Chem Soc Jpn) 1364
9. Iwamoto S, Tanakulrungsank W, Inoue M, Kagawa K, Praserthdam P (2000) J Mater Sci Lett 19:1439
10. Iwamoto SH, Iwamoto SE, Inoue M, Uemura S, Kagawa K, Tanakulrungsank W, Praserthdam P (2000) Ceram Trans 115:643
11. Iwamoto SH, Iwamoto SE, Inoue M, Yoshida H, Tanaka T, Kagawa K (2005) Chem Mater 17:650
12. Iwamoto S, Saito K, Inoue M, Kagawa K (2001) Nano Lett 1:417
13. Odenbrand CUI, Andersson SLT, Andersson LAH, Brandin JGM, Busca G (1990) J Catal 125:541
14. Stakheev AY, Shpiro ES, Apijok J (1993) J Phys Chem 97:5668
15. Muilenberg GE (1979) Handbook of X-ray photoelectron spectroscopy. Perkin-Elmer Corporation, Minnesota, p 45
16. Parks GA (1965) Chem Rev 65:177
17. Wu T, Liu G, Zhao J, Hidaka H, Serpone N (1998) J Phys Chem B 102:5845
18. Vinodgopal K, Kamat PV (1992) J Phys Chem 96:5053